

## OPTIMIZATION OF INSTRUMENT RESPONSE AND RESOLUTION OF STANDARD- AND HIGH-SPEED POWER COMPENSATION DSC Benefits for the study of crystallization, melting and thermal fractionation

M. F. J. Pijpers<sup>1,2</sup> and V. B. F. Mathot<sup>1,2\*</sup>

<sup>1</sup>SciTe, Ridder Vosstraat 6, 6162 AX Geleen, The Netherlands

<sup>2</sup>Laboratory of Macromolecular Structural Chemistry, Division of Molecular and Nanomaterials, Department of Chemistry Katholieke Universiteit Leuven, Celestijnenlaan 200F, 3001 Heverlee, Belgium

Normally, for Standard DSC, the PerkinElmer power-compensation setting is the low dynamic range mode (LDRM). In this mode, a noise filter is applied to decrease the noise-to-signal ratio, which concomitantly gives rise to a delay in time of the signal measured. In case the signal is expected to be of high intensity – experienced for instance at high scan rates using High Performance DSC (HPer DSC) – the noise filtering could be diminished by which the associated delay in time would be less, leading to a faster response of the instrument, also resulting in an improved resolution. In fact, such can be realized using the faster noise filter of the high dynamic range mode (HDRM) available for the Pyris 1 and Diamond DSCs, which DSCs are both equipped with the HyperDSC™ technique (HyperDSC being the commercial version of HPer DSC). The improvement in response is maximal for high rates like 100–500°C min<sup>-1</sup> but even at low rates like 10°C min<sup>-1</sup> it is still significant. Thus, taking advantage of HDRM, low-molar substances like indium and 4,4'-azoxyanisole show appreciable increasing height-to-width ratios for signals caused by crystallization, melting and the crystal <> liquid crystal transition respectively. Another advantage, the faster realization of steady state after the starting of the DSC, is of help in case of overlapping starting and transition signals during dynamic crystallization and melting, and during isothermal crystallization as elucidated for a HDPE. For 4,4'-azoxyanisole and for an ethylene-propylene copolymer having a broad melting range, it is shown that such faster response leads to a still better resolution with respect to temperature, even at high scan rates.

Thus, the peaks belonging to the crystal-to-liquid crystal and the liquid crystal-to-isotropic liquid transitions of 4,4'-azoxyanisole were completely resolved while a thermal fractionation of the copolymer by the successive self-nucleation and annealing (SSA) technique with good resolution has been realized, both using rates as high as 200°C min<sup>-1</sup>.

**Keywords:** annealing, cooling rate, crystallization, fast scanning rate, heating rate, high performance DSC (HPer DSC), high-speed calorimetry, HyperDSC™, melting, noise filter, power compensation, resolution, sensitivity, thermal fractionation, thermal lag

### Introduction

Recently, high-performance DSC (HPer DSC) has been introduced [1] as a tool for measuring at higher (controlled, constant) scan rates – typically up to 500°C min<sup>-1</sup> in cooling and heating – than possible by 'Standard' DSC, which operates typically at rates around 10°C min<sup>-1</sup>. The commercial version of HPer DSC is available under the name HyperDSC: both the Pyris 1 and Diamond DSCs are equipped with the HyperDSC™ technique [2].

Advantages found hitherto for HPer DSC are:

- increased sensitivity at higher rates
- increased productivity
- better possibilities to study the kinetics of processes
- study of reorganization phenomena; hindering or suppression of undesired reorganization pheno-

mena like cold- and recrystallization; solid–solid transformations

- matching rates occurring in daily practice
- mimicking of rates during processing, like in case of extrusion, injection molding
- measuring on minute amounts – from milligram down to microgram level – of materials and substances, such as coatings, contaminants; fractions and as used in combinatorial chemistry experiments
- capable of performing approximately 100 heat-cool-heat measurements a day for combinatorial chemistry research
- possibility of performing quantitative measurements (high performance DSC), including heat capacity measurements, and
- all that – for both low and high scan rates – utilizing one and the same device.

\* Author for correspondence: vincent.mathot@scite.eu

Being able to choose optimum scan rates and scan rate combinations for tackling a problem under study is an important advantage of HPer DSC. It illustrates that HPer DSC is not meant to replace Standard DSC, but should be seen as a complementary capability for researchers by facilitating the use of both low and high heating rates, even using the same equipment.

A recurrent question in the field of high-speed calorimetry is whether the response (the shape of the heat flow rate curve as function of temperature, which comprises influences like the sensitivity of the measuring cell, the effectiveness of power compensation, etc.) and resolution (the ability to measure two transitions which occur close to each other with respect to temperature, as separate, at least distinct heat flow rates) are not much worsened by measuring at high rates. Of course, if one would measure at high rates under the same conditions without precautions taken, the answer would be confirmative: high rates would delay the calorimeter's response; not only would the thermal lag be increased, also the curves would be broadened by which the resolution would be poorer.

To avoid this undesirable situation, minimization of thermal lag is realized by improving the heat transfer between instrument and sample using Aluminum foil [1] or a thin-foil sample pan, wrapping the sample entirely. The remaining shift in onset temperature caused by the instrumental thermal lag – different for each scan rate – is corrected using a proper scan-rate dependent temperature calibration [1, 3, 4]. To minimize the thermal gradient within the sample it was suggested to decrease the sample mass with increasing scan rate [1, 3].

These actions aim to ensure that the shape of the DSC curve does not change appreciably whether one measures at a normal scan rate of  $10^{\circ}\text{C min}^{-1}$  or at a higher rate, like  $50^{\circ}\text{C min}^{-1}$  [1] – of course if the nature and the kinetics related of the phenomenon studied do not change. The way to optimize the response at much higher rates, like  $200^{\circ}\text{C min}^{-1}$ , is the topic of this paper, while in addition the resolution at such high scan rates will be discussed.

## Experimental

Almost all measurements were performed with a PerkinElmer Diamond DSC having software version 7.0. According to the information provided by PerkinElmer, in case of the low data range mode (LDRM) or normal data range mode, the data range amounts to  $\pm 320$  mW, while in the high data range mode (HDRM), the data range is  $\pm 720$  mW. Because the word 'dynamic' covers the issue better than 'data', from here on the 'D' in LDRM and HDRM stands for

dynamic: LDRM and HDRM. The CryoFill system used for cooling by liquid nitrogen provides a very effective heat sink. Helium was used as the gas atmosphere surrounding the sample containers. To promote optimal thermal contact between the sample and instrument, thin aluminum foil and thin aluminum foil sample pans (PerkinElmer no. N5203115) have been used to wrap the sample. Low sample masses are used, typically around 1 mg and lower.

Temperature calibrations using the 'deduced' onset of indium – being decided as the first 'appreciable' departure from the baseline on the scale of the plot – have been performed for each scan rate used and for isothermal stays, and checked with the onset of melting of water. Power calibrations were performed using indium. A furnace calibration was performed in which the furnace temperature and sample temperature are equaled. It turns out that the findings reported for the Diamond DSC also apply to the Pyris 1 DSC.

## Results and discussion

### *High- and Low-DRM*

During research on applications of HPer DSC, we explored a seldom used option available for the PerkinElmer Pyris 1 and Diamond DSCs: HDRM, having a dynamic range of  $\pm 720$  mW. Normally, the DSC instrument's setting is in the LDRM or normal dynamic range mode, with a dynamic range of  $\pm 320$  mW. The HDRM was originally intended for use in case a large dynamic range for measuring is needed, e.g. like for measurements on explosives. In LDRM, the noise-to-signal ratio is decreased by applying a noise filter; in HDRM a faster noise filter is used. Figure 1 shows the resulting differences in noise level for LDRM and HDRM using the Diamond DSC in heating at  $200^{\circ}\text{C min}^{-1}$ . A drawback of applying LDRM compared with HDRM in order to have less noise is the concomitant larger delay of the instrument response and by that an increase of the thermal lag. In case the signal expected is anticipated to be of high intensity – e.g. high heat flow rates because of fast crystallization/melting or fast heat exchange in general, or in case of strongly-changing signals as usually experienced at high scan rates – the noise level is of less importance (if at all) and the filtering can be minimized, by which the instrument response is slowed down less, resulting in a decrease of the thermal lag. That is exactly what is happening in case the range of the Pyris 1 or Diamond DSC is set to HDRM.

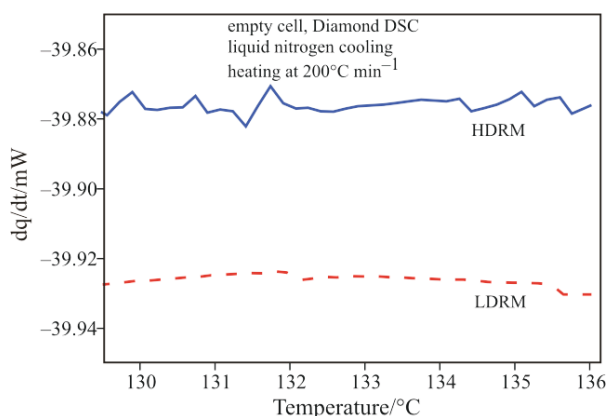


**Fig. 1** Empty cell measured in heating at  $200^{\circ}\text{C min}^{-1}$ , using LDRM and HDRM settings of the Diamond DSC showing characteristic differences in noise-to-signal levels

#### Application of the HDRM to indium

In Fig. 2, the difference between LDRM and HDRM settings is elucidated with respect to the resulting heat flow rates as function of temperature for an indium sample heated at  $200^{\circ}\text{C min}^{-1}$ . The melting of the 2.18 mg sample during heating is seen to occur within approx.  $13^{\circ}\text{C}$  ( $\sim 4$  s) using the HDRM (with a slight ‘overshoot’ around  $172^{\circ}\text{C}$ ), while it amounts to approx.  $21^{\circ}\text{C}$  using the LDRM, which is an appreciable higher number. Thus, HDRM results in a much faster instrument response compared to LDRM and by that a narrower melting curve is realized.

In an analogous way, Fig. 3 shows the results for indium at an even higher heating rate of  $500^{\circ}\text{C min}^{-1}$ . Clearly, melting is seen to be finished within approx.  $31^{\circ}\text{C}$  ( $\sim 3.5$  s) – compare with  $13^{\circ}\text{C}$  ( $\sim 4$  s) in case of  $200^{\circ}\text{C min}^{-1}$  – using HDRM, while using LDRM the signal returns to its baseline at much higher temperatures.

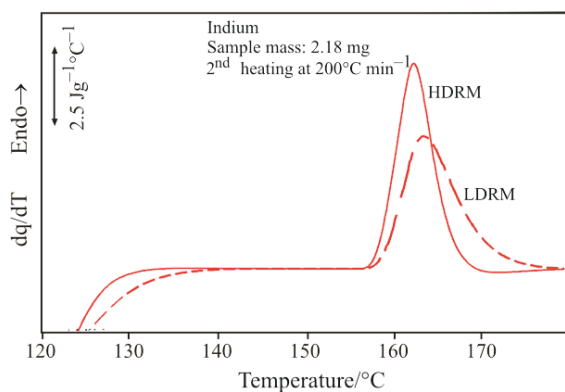


**Fig. 2** Indium measured in heating at  $200^{\circ}\text{C min}^{-1}$  after cooling at  $100^{\circ}\text{C min}^{-1}$ , using LDRM and HDRM settings of the Diamond DSC

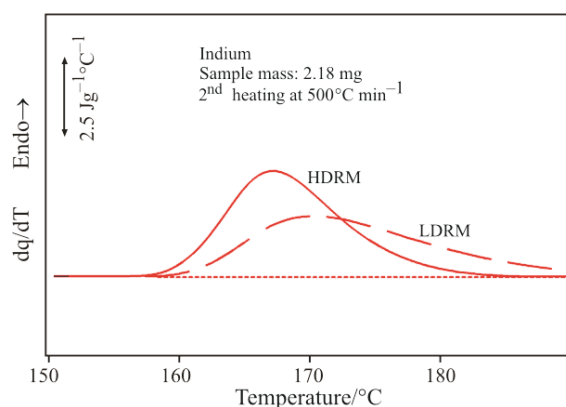


**Fig. 3** Indium measured at  $500^{\circ}\text{C min}^{-1}$  heating after cooling at  $500^{\circ}\text{C min}^{-1}$ , further as in Fig. 2

It is also interesting to have a look to cooling curves. The crystallization of indium serves the purpose to explore the influence of HDRM and LDRM on the cooling curve shape well. As is seen in Fig. 4, using HDRM is again profitable: the height-to-width ratio of the DSC curve is markedly increased, reflecting a much faster instrument response compared with the curve measured in LDRM.

It has to be remarked that it should not be taken for granted that the instrument should behave the same in cooling as in heating. In cooling the surroundings of the sample container play a much more important role than in heating, and of particular importance are the purge gas and the temperature control of the surroundings: the effectiveness of the heat sink; the temperature difference between the heat sink and sample container, etc., all as related to the cooling rate programmed. As an example, while in case of the  $200^{\circ}\text{C min}^{-1}$  cooling (Fig. 4) and  $500^{\circ}\text{C min}^{-1}$  heating (Fig. 3) experiments good results have been obtained, cooling at  $500^{\circ}\text{C min}^{-1}$  does not give curves of which the signal returns to its baseline above  $110^{\circ}\text{C}$ . This is not caused by a failure to achieve and maintaining  $500^{\circ}\text{C min}^{-1}$ : this very high cooling rate as measured by the sensor temperature

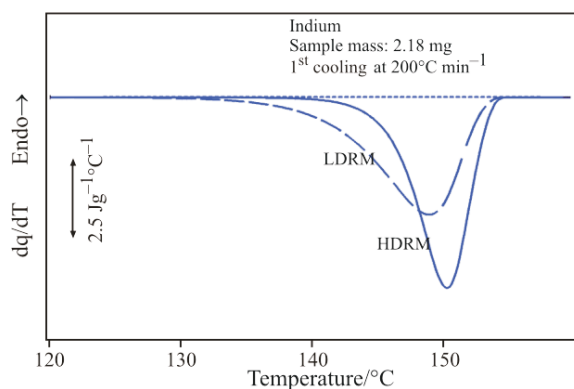


**Fig. 4** Indium measured during cooling at  $200^{\circ}\text{C min}^{-1}$ , using LDRM and HDRM of the Diamond DSC

turns out to be constant down to the temperature mentioned.

One could pose the question: is HDRM always preferred above LDRM? As stated at the beginning, HDRM is of use when a large dynamic range for measurement is needed. In principle, if such a situation is not met, there is no reason to use HDRM. However, it turns out that even in such cases there are slight advantages of using HDRM. Examples of 'low-dynamic range' signals, where HDRM still offers a slight advantage, are given in Figs 5a and b, for heating and cooling at  $10^{\circ}\text{C min}^{-1}$  of an indium sample respectively. Notice again the slight overshoots in both curves.

As a conclusion, it is advisable to stick to one DRM setting if the signal-to-noise level permits – which is usually the case – and therefore to the use of HDRM. However, it might not be completely clear beforehand to what extent HDRM will be an

improvement over LDRM: it is worthwhile to find out for a specific case at hand by comparing both ways of instrument settings.

As illustrated in Fig. 1, of course an increase is seen of the noise level using HDRM instead of LDRM. However, it turns out that usually the signal-to-noise ratio does not form any obstacle, and that only in rare cases the need of considering the use of LDRM because of a not-acceptable noise level is opportune. An example in mind is when HPer DSC on SEC fractions is performed, in which combination of techniques the sample masses used are very low (down to the microgram level) and consequently curves can be noisy [5].

From the foregoing it is striking that for HDRM and LDRM the 'deduced onsets' coincide, while the 'extrapolated onsets' do not, especially not at high rates, leading to discrepancies amounting to several degrees in the latter case, Figs 2–4. This information is useful with respect to temperature calibration procedures in case of high scanning rates [3]. In principle, the extrapolated onset is usually easy to determine which is why it is often the preferred way of determination of the melting point of indium. However, in order to ensure consistency in case of possible switching between HDRM and LDRM, it is inevitable from the present study that the 'deduced onset' should be used for temperature calibration.

Of interest is the fact that starting signals (starting of a cooling or heating run) are affected too by the choice of DRM, Fig. 2: here in heating the steady state is reached faster for HDRM, which is of help at high rates to avoid the starting signal interfering with the phenomenon to be studied.

An excellent application of this finding is of course the investigation of isothermal crystallization as function of time, followed by a heating run. A close control of temperature throughout the temperature–time ramps of the investigation is of crucial importance: firstly, during fast cooling to a specific crystallization temperature there should be no or hardly any overshoot; secondly, subsequently the signal should quickly equilibrate at the crystallization temperature in order to be able to follow isothermal crystallization right from its start; and thirdly, preferably, it should be possible in the final heating step to separate the starting signal and the measuring signal during heating as much as possible.

Figure 6 gives an example of the advantage of using HDRM in case of a HDPE with respect to the second aspect: quick equilibration and isothermal crystallization at  $121.6^{\circ}\text{C}$ , by which the instruments signal interferes less with the measuring signal than in case of LDRM. The subsequent heating curve (not

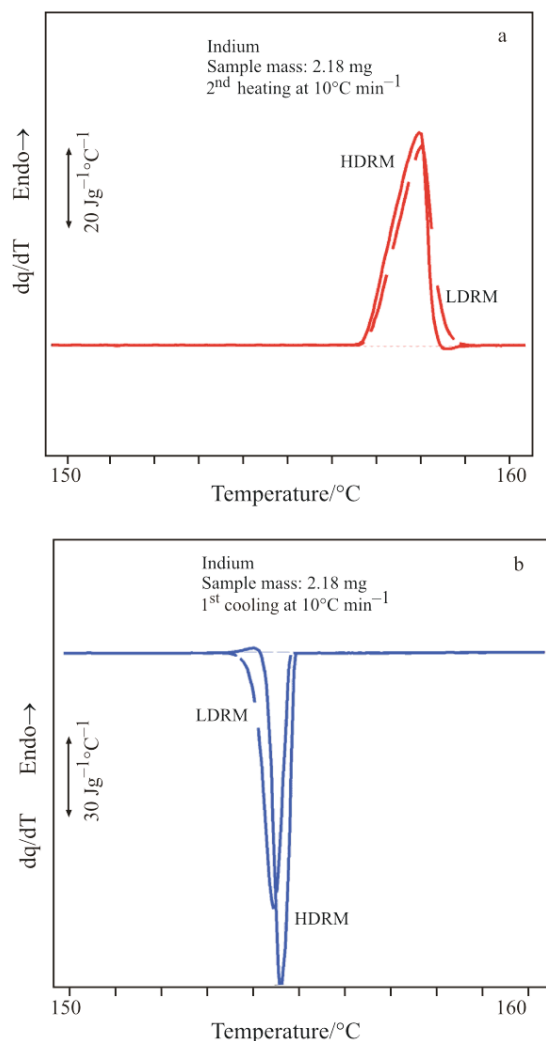


**Fig. 5** Diamond DSC a – heating and b – cooling curves at  $10^{\circ}\text{C min}^{-1}$  of indium in HDRM and LDRM. Notice the different heat flow rate scales in a and b

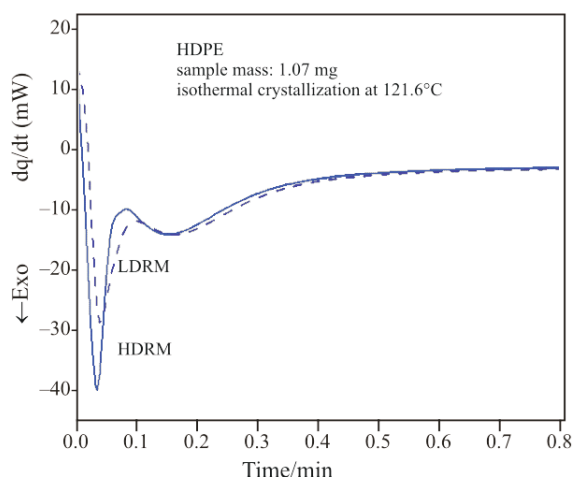


**Fig. 6** Isothermal crystallization in LDRM and HDRM at 121.6°C of a 1.07 mg HDPE sample subsequent to cooling at 200°C min<sup>-1</sup> from 200°C after 3 min waiting time at that temperature

shown here) using HDRM shows less overlap with the starting signal compared to LDRM as expected.

#### *Of use for other substances?*

If it works for indium, will it also work for other substances, including pharmaceuticals? And, in the extreme, could it also be of use for substances like polymers, which often show broad crystallization and melting transitions? If the delay in time caused by noise-filtering is shortened using HDRM, giving rise to concomitant narrowing of curves also resulting in an improved resolution, one would expect at least one potential beneficial influence: the possibility of keeping a peak separated from other ones when using high scan rates. Especially for polymers and pharmaceuticals, this would be of interest because often multiple peaks are found.

To test out whether the resolution improves appreciably, working on calibration standards would be the first choice. However, the 4,4'-azoxyanisole sample, used for the so-called TAWN resolution and sensitivity tests [6], was thought [3] not to be usable at heating rates higher than 200°C min<sup>-1</sup> because the low-temperature peak (crystal-to-liquid crystal transition: extrapolated onset of 115.85°C at 10°C min<sup>-1</sup>) shifts to higher temperatures and then overlaps with the high-temperature peak (liquid crystal-to-isotropic liquid transition: peak temperature of 135.85°C at 10°C min<sup>-1</sup>). However, the measurements in [3] were done in LDRM, and it is to be expected that in this case again the HDRM could stretch the limits.

Figure 7a demonstrates a remarkable improvement of the quality of the cooling curve at

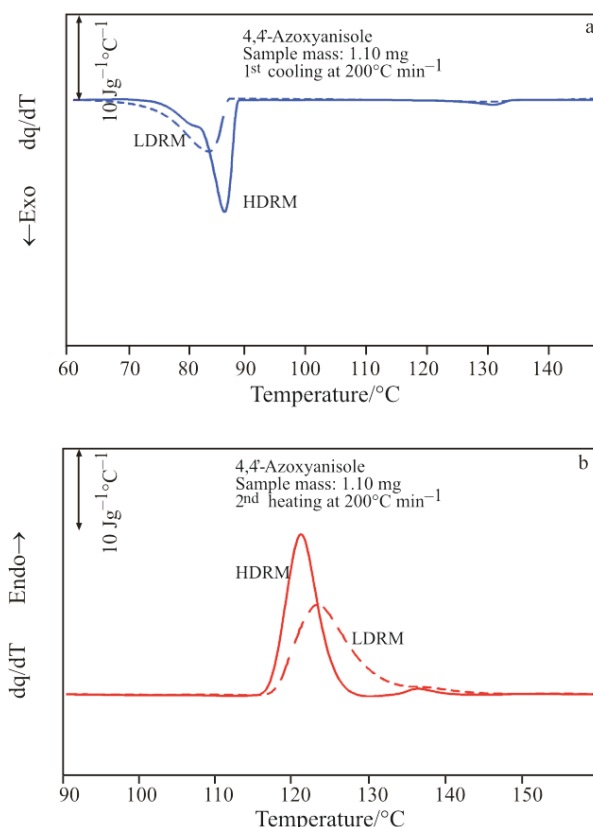


**Fig. 7** a – Cooling curves from 180 to 20°C – but shown in a relevant temperature range – at 200°C min<sup>-1</sup> for a 1.10 mg 4,4'-azoxyanisole sample in LDRM and HDRM; b – heating curves at 200°C min<sup>-1</sup> shown in a limited range, further as in a

200°C min<sup>-1</sup> of a 4,4'-azoxyanisole sample by switching from LDRM to HDRM. The isotropic liquid to liquid crystal transition is seen much better, while there is even a shoulder emerging at the low-temperature side of the liquid crystal to crystal transition, due to the improved response/resolution. In Fig. 7b, in heating at 200°C min<sup>-1</sup>, again an extraordinary improvement is seen. A direct result is the 'return' of the two peaks in case of HDRM while in LDRM it is noticed that the two peaks are merging because of 'smearing' of their respective signals. Because the two peaks are well separated – the signal is seen to return fully to the baseline in between – also still higher heating rates are usable. Thus, the high-temperature peak (liquid crystal <> isotropic liquid transition, peak temperature) is still suited to be used for calibration in both cooling and heating, contrary to earlier expectation. By that for high-speed/high performance calorimetry the range of secondary calibration standards is extended: the ones studied before – the liquid crystalline substances M24, HP-53, BCH-52 – have been found useful [3], while now 4,4'-azoxyanisole can be added too: all being substances with no or very small supercoolings. Also

– as has been explained in [3] – the symmetry of the DSC instrument used with respect to its cooling and heating behavior can be checked with these substances. If an asymmetry is found, separate calibrations for heating and cooling are of necessity.

Interestingly, if the high-speed/high performance calorimeters are being improved with respect to response and resolution, it is to be expected that the secondary calibration substances still will be useful also at much higher scan rates. Finally, in principle, it is likely that also ultra-fast chip calorimeters [7] will benefit from these substances.

As a result, 4,4'-azoxyanisole can still be used for resolution and sensitivity tests. Though at the moment there are no instruments to be compared using such tests, it is hoped and anticipated that more instrument manufacturers will enter the high-speed/high performance calorimetry market, as the benefits of this kind of instrumentation – seen as complementary to so-called 'standard DSC' – in research and development are obvious.

Alternatively to the use of 4,4'-azoxyanisole, one could mix substances, melting with a few °C difference, or study a substance showing transitions a few degrees apart, but such substances are not readily available and certainly not certified. Interesting enough it turns out to be possible to use polymers for the purpose of a resolution test in an elegant and easy way, as will be discussed in the next sections.

#### *Application to polymers: thermal fractionation*

Macromolecular substances are known for their metastability: an extreme susceptibility of their crystallization and melting behavior to the way they are treated thermally. Low or high cooling and/or heating rates; isothermal stays and annealing steps and combinations thereof usually significantly influence the way crystallites are formed and melt subsequently. As a result, reorganization phenomena like cold crystallization; recrystallization; solid-state transformations etc. occur frequently instead of being exceptional.

An extreme example is given in Fig. 8, showing one of the first power compensation DSC measurements done on a polymer by Gray and Casey in 1964 [8]. The multiple peaks illustrate that multiple-step annealing at different temperatures can result in crystallite perfectioning and possible larger dimensions. Because of the increased thermodynamic stability, each annealing step results in a local shift of the melting of a class of crystallites to slightly higher temperatures (causing a peak or 'hill'), leaving a 'valley' around the annealing temperature. Repeating the annealing step at different temperatures causes the

A. P. Gray and K. Casey, *Polym. Lett.*, 2 (1964) 381–388  
Fusion curve of an ethylene-6-m% butene copolymer after step-wise annealing. DSC-1b curve on heating at  $18^{\circ}\text{C min}^{-1}$ . The multiple peaks refer to crystals of different stability produced by the thermal pretreatment: annealing for 1 min each, in steps of  $5^{\circ}\text{C}$ , started at the highest temperature. Before and between annealings the sample was quenched to ambient temperature

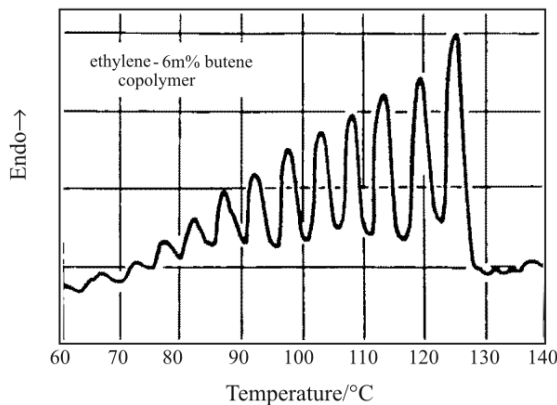


**Fig. 8** Metastability: 'thermal fractionation' by step-wise annealing of an ethylene-butene copolymer (6 mol% of butene) resulting in multiple peaks. Reprinted from [8] with permission of John Wiley & Sons, Inc.

multiple-peaked curve, which is a kind of histogram reflecting the melting point distribution after successive annealing steps related to a distribution (a discrete distribution – but an artificial one because it is determined by the limited number of annealing steps) of crystallites differing in perfection and/or dimensions. In fact, an ordinary DSC curve can be seen as a melting point distribution which is continuous because of the almost 'un'limited number of annealing steps.

Therefore, using this kind of treatment one should focus on the influence of the annealing and cooling/heating procedure on crystallite perfection and dimensions, and see whether there is any advantage of enforcing a discrete distribution over a continuous one. However, this is not the topic of the present paper and therefore the measurements and discussion will be limited to the technicalities of the procedure mentioned, following the general opinion as found in literature.

The capability of modern DSCs to closely follow such complicated temperature-time ramps as shown in Fig. 8 has led to their use for so-called thermal fractionation techniques which '...offer quick and practical ways to evaluate chain heterogeneities in semicrystalline thermoplastic materials by employing carefully designed thermal cycles in a DSC' [9]. Thus, in literature the opinion is found that thermal fractionation provides an alternative to laborious and time-consuming fractionation techniques like TREF, Crystaf, etc.. However, it uses crystallization and melting of the pure polymer instead of a polymer-solvent system, causing problems regarding the

diffusion of the long chains. This in turn will cause local, forced cocrystallization of chain segments which do not have a strict similarity with respect to the microstructure, by which the fractionation on the basis of chain microstructure via crystallization from the melt intrinsically will be less effective than in case of using a solvent.

The route Gray *et al.* followed, is nowadays modified into the successive self-nucleation and annealing (SSA) technique [9]. Figure 9 illustrates a recent example exploring the influence of various scan rates on the performance/efficiency of the SSA technique. Müller *et al.* conclude that SSA can be performed employing scan rates as fast as  $50^{\circ}\text{C min}^{-1}$  using a PerkinElmer Pyris 1 equipped with an intracooler device; and that the resolution at high rates is almost identical to the resolution at low rates as long as the sample mass is adjusted concomitantly, following the recommendation given in [1]. The authors conclude that the use of  $50^{\circ}\text{C min}^{-1}$  for all heating and cooling rates leads to ‘...the fastest thermal fractionation time ever reported in the literature and with equivalent resolution to usual conditions involving  $10^{\circ}\text{C min}^{-1}$ .’

#### Using HDRM for polymers

Using the PerkinElmer Pyris 1 and Diamond DSCs it is possible to work at even higher rates than reported in Fig. 9: see the experiment in Fig. 10 where the heating rate has been increased to  $200^{\circ}\text{C min}^{-1}$ . In order to make the high cooling rate feasible in the temperature range chosen, helium was employed as purge gas. The homogenous ethylene-propylene copolymer, code EP 203, used has a propylene mol% of 17.4, and  $M_n^*$ ;  $M_w^*$ ;  $M_z^*$  of 25, 170, 320  $\text{kg mol}^{-1}$ , respectively. The crystallization and melting behavior of the copolymer as studied by standard DSC has been reported in [10].

Within the scope of the present paper, it is not the further reduction in time which is of importance (in fact, the time of the isothermal stays now becomes the limiting factor), but the fact that the experiment demonstrates the capability of the instrument to maintain a high resolution.

For the SSA measurements, the starting temperature was  $150^{\circ}\text{C}$  with an isothermal stay of 3 min; the sample (having a mass of 0.50 mg) was then cooled at  $100^{\circ}\text{C min}^{-1}$  to  $-100^{\circ}\text{C}$ ; subsequently it was heated at  $200^{\circ}\text{C min}^{-1}$  to isothermal stays at 79.4, 74.4, 69.4, 64.4, 54.4, 44.4, 24.4 and  $4.4^{\circ}\text{C}$  (the temperature calibration for rate zero, providing corrected values, was done afterwards based on the uncorrected, programmed values: 73, 68, 63, 58, 48, 38, 18 and  $-2^{\circ}\text{C}$ ), with isothermal waiting times of 1 min, and in

A. J. Müller and M. L. Arnal, Prog. Polym. Sci., 30 (2005) 559–603  
At  $50\text{ K min}^{-1}$  the quality of the fractionation is still very good for HPB and the fractionation time has been reduced to only 78 min

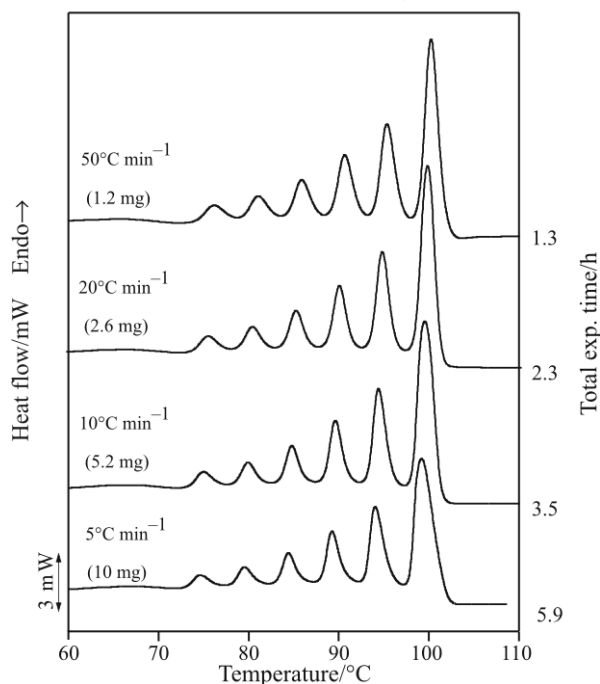


**Fig. 9** Hyper DSC (PerkinElmer Pyris 1 with intracooler) used for SSA (see text) on a hydrogenated polybutadiene (HPB) to further reduce fractionation time. Reprinted from [9] with permission of Elsevier

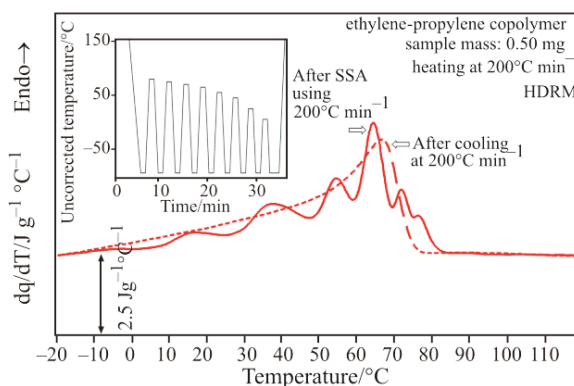


**Fig. 10** Heating curves shown in between  $-20$  and  $120^{\circ}\text{C}$  (but measured in between  $-100$  and  $150^{\circ}\text{C}$ ) of a homogeneous ethylene-propylene copolymer (17.4 mol% of propylene). --- Heating at  $200^{\circ}\text{C min}^{-1}$  after cooling at  $200^{\circ}\text{C min}^{-1}$ ; and — heating after a SSA temperature-time ramp using  $200^{\circ}\text{C min}^{-1}$ ; see inset and text. PerkinElmer Diamond Hyper DSC in HDRM, with liquid nitrogen cooling and helium purge gas. The aluminum foil containing the sample (of mass 0.50 mg) was flattened to a thickness of 0.17 mm

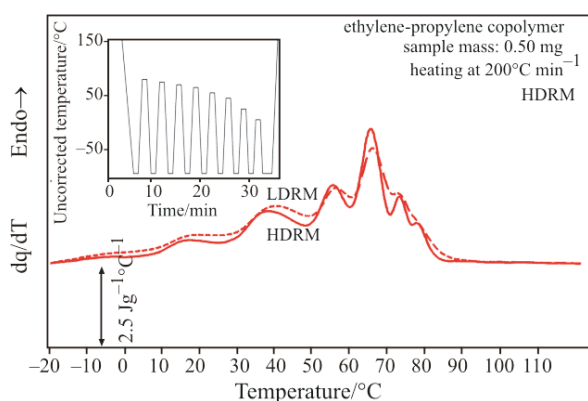
between cooled and heated at the same rates to and from  $-100^{\circ}\text{C}$  respectively, again with isothermal waiting times of 1 min – save a 2 min applied for the last one – before the final heating at  $200^{\circ}\text{C min}^{-1}$  was performed resulting in the solid curve plotted in

Fig. 10. All temperatures were properly corrected for the scan rate of  $200^{\circ}\text{C min}^{-1}$ , and also, separately, as mentioned, the isotherms (scan rate zero  $^{\circ}\text{C min}^{-1}$ ). Note that the isothermal stays at  $64.4$  and  $79.4^{\circ}\text{C}$  (compare the temperatures of the valleys in the figure) do not seem to result in separate valleys/peaks.

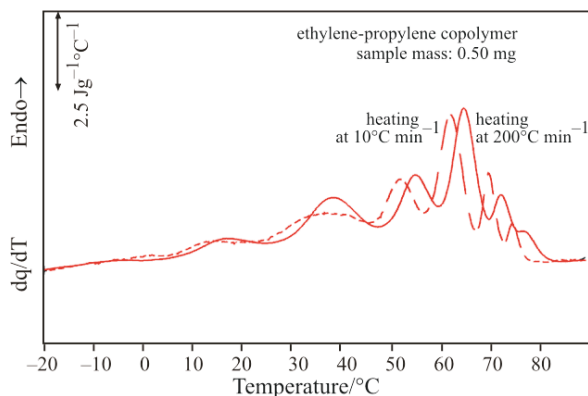
Clearly the resolution is excellent: be aware of that in heating at  $200^{\circ}\text{C min}^{-1}$  it just takes a few seconds to bridge two peaks. For comparison, in the figure also the 2<sup>nd</sup> heating curve at  $200^{\circ}\text{C min}^{-1}$  after cooling at the same rate is presented. Clearly, the modification of the melting temperature distribution by the SSA treatment is appreciable.

Figure 11 compares HDRM and LDRM for the same copolymer, following exactly the same SSA temperature-time ramp as in Fig. 10. LDRM gives useful results but obviously, HDRM gives an even better resolution.

As in Fig. 9, it is of interest to compare the final heating curves after applying SSA as outlined in Fig. 10, using two different scan rates throughout:  $200^{\circ}\text{C min}^{-1}$  and a typical standard rate of  $10^{\circ}\text{C min}^{-1}$ , Fig. 12. Compared to the curve at



**Fig. 11** Final heating curves after applying SSA to a homogeneous ethylene-propylene copolymer in HDRM and LDRM, further as in Fig. 10



**Fig. 12** Final heating curves after applying SSA to a homogeneous ethylene-propylene copolymer, at  $10$  and  $200^{\circ}\text{C min}^{-1}$  throughout, further as in Fig. 10

$10^{\circ}\text{C min}^{-1}$ , the very high heating rate of  $200^{\circ}\text{C min}^{-1}$  gives a usable result as well. Looked upon in detail, at  $200^{\circ}\text{C min}^{-1}$ , the resolution is seen to be slightly better after isothermal stays at the low temperatures of  $4.4$  and  $24.4^{\circ}\text{C}$ , while it is slightly worse after stays at the high temperatures of  $69.4$  and  $74.4^{\circ}\text{C}$ .

## Conclusions

PerkinElmer power-compensation HyperDSC curves, as obtained by both Diamond DSC and Pyris 1 DSC's, show good power compensation in the normal dynamic range mode or LDRM. However, because usually the noise level is low, it is recommended to use the HDRM instead; in which case a reduced noise filtering is applied compared to LDRM. Then, the delay in time because of the filtering is decreased; the signal shows a faster response, and as an outcome, the resulting DSC curves have increased height-to-width ratios and improved resolution. This applies to both heating and cooling. The effect is maximal at high rates but still significant at low rates like  $10^{\circ}\text{C min}^{-1}$ . In addition, the DSC reaches steady state faster, which is of advantage in case of overlapping of the starting signal and the phenomenon studied, like in dynamic cooling or heating, and in isothermal crystallization as illustrated for a HDPE sample. In HDRM, 4,4'-azoxyanisole turns out to be still usable as a secondary calibrant at rates as high as  $200^{\circ}\text{C min}^{-1}$  and also as a substance for a resolution and sensitivity test at such rates. In general, secondary calibration substances like the liquid crystalline M24, HP-53, BCH-52 and 4,4'-azoxyanisole will be useful for high-speed/high performance calorimeters also in case of much higher cooling and heating rates like those realized by ultra-fast chip calorimeters. An extreme application of the use of HDRM is in thermal fractionation experiments in which a good resolution is realized for the many peaks – resulting from successive annealing steps – even at heating rates as high as  $200^{\circ}\text{C min}^{-1}$ .

## Acknowledgements

The support provided by PerkinElmer, Shelton, CT, USA is appreciated.



**References**

- 1 T. F. J. Pijpers, V. B. F. Mathot, B. Goderis, R. L. Scherrenberg and E. van der Vegte, *Macromolecules*, 32 (2002) 3601., *Handbook of Therm. Anal. Cal.* (Series Editor: Patrick Gallagher); Vol. 5: Recent Advances, Techniques and Applications (Editors: Michael Brown and Patrick Gallagher); Chapter 8. Vincent B. F. Mathot, Geert Vanden Poel and Thijs F. J. Pijpers, Benefits and Potentials of High performance Differential Scanning Calorimetry (HPer DSC) (2008) 269-297.
- 2 V. B. F. Mathot, G. Vanden Poel and T. F. J. Pijpers, *American Laboratory*, 38 (2006) 21. See also recent Webcasts by V. B. F. Mathot, downloadable for free via [www.hyperdsc.com](http://www.hyperdsc.com) and [www.scite.eu](http://www.scite.eu).
- 3 G. Vanden Poel and V. B. F. Mathot, *Thermochim. Acta*, 446 (2006) 41.
- 4 G. Vanden Poel and V. B. F. Mathot, *Thermochim. Acta*, 461 (2007) 107.
- 5 N. Luruli, T. Pijpers, R. Brüll, V. Grumel, H. Pasch and V. Mathot, *J. Polym. Sci. Part B: Polym. Phys.*, 45 (2007) 2956.
- 6 P. J. van Ekeren, C. M. Hol and A. J. Witteveen, *J. Thermal Anal.*, 49 (1997) 1105.
- 7 A. A. Minakov, S. A. Adamovsky and C. Schick, *Thermochim. Acta*, 432 (2005) 177.
- 8 A. P. Gray and K. Casey, *J. Polym. Sci. Part B: Polym. Lett.*, 2 (1964) 381.
- 9 A. J. Müller and M. L. Arnal, *Prog. Polym. Sci.*, 30 (2005) 559.
- 10 S. Vanden Eynde, V. Mathot, M. H. J. Koch and H. Reynaers, *Polymer*, 41 (2000) 3437.

---

DOI: 10.1007/s10973-007-8924-8